ACS APPLIED MATERIALS & INTERFACES

Research Article

www.acsami.org

Highly Efficient Inverted Polymer Solar Cells Based on a Cross-linkable Water-/Alcohol-Soluble Conjugated Polymer Interlayer

Kai Zhang,[†] Chengmei Zhong,[†] Shengjian Liu,[†] Cheng Mu,[‡] Zhengke Li,[‡] He Yan,*[,‡] Fei Huang,*[,†] and Yong Cao[†]

[†]Institute of Polymer Optoelectronic Materials and Devices, State Key Laboratory of Luminescent Materials and Devices, South China University of Technology, Guangzhou, Guangdong 510641, P. R. China

[‡]Department of Chemistry, The Hong Kong University of Science and Technology, Clear Water Bay, Kowloon, Hong Kong

Supporting Information

ABSTRACT: A cross-linkable water/alcohol soluble conjugated polymer (WSCP) material poly[9,9-bis(6′-(*N*,*N*-diethylamino)propyl)-fluorene-*alt*-9,9-bis(3-ethyl(oxetane-3-ethyloxy)-hexyl) fluorene] (PFN-OX) was designed. The cross-linkable nature of PFN-OX is good for fabricating inverted polymer solar cells (PSCs) with well-defined interface and investigating the detailed working mechanism of high-efficiency inverted PSCs based on poly[4,8-bis(2-ethylhexyloxyl)benzo[1,2-b:4,5-b′]dithio-phene-2,6-diyl-*alt*-ethylhexyl-3-fluorothithieno[3,4-*b*]thiophene-2-carboxylate-4,6-diyl] (PTB7) and (6,6)-phenyl-C71-butyric acid methyl ester ($PC_{71}BM$) blend active layer. The detailed working mechanism of WSCP materials in high-efficiency PSCs were studied and can be summarized into the following three effects: a) PFN-OX tunes cathode work function to enhance open-circuit voltage (Voc); b) PFN-OX dopes $PC_{71}BM$ at interface to facilitate electron extraction; and c) PFN-OX extracts electrons and blocks holes to enhance fill factor (FF). On the basis of this understanding, the hole-blocking function of the PFN-OX interlayer was further improved with addition of a ZnO layer between ITO and PFN-OX, which led to inverted PSCs with a power conversion efficiency of 9.28% and fill factor high up to 74.4%.

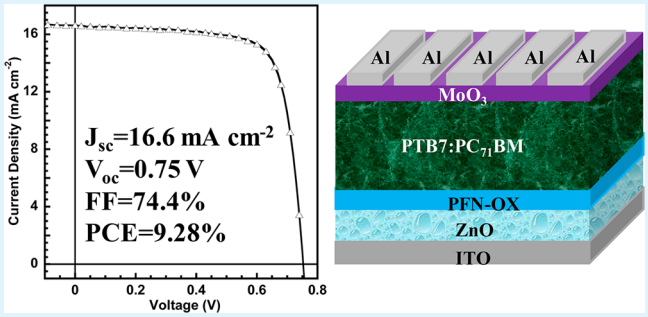

KEYWORDS: *water/alcohol soluble, cathode interlayer, inverted polymer solar cells, interfacial doping, hybrid interlayer*

INTRODUCTION

The polymer solar cells (PSCs) have attracted considerable research attention from both academia and industry over the past decade because of such advantages as low-cost fabrication and mechanical flexibility.[1,2] Recently, single-junction PSCs have broken a power conversion efficiency (PCE) record of 9%,[3−5] whereas the record PCE for tandem organic solar cells broke 10%.[6,7] Of particular interest are the so-called inverted structure PSCs, which exhibit superior efficiency and stability compared with their conventional structure counterparts.[3,8−11] A key component of inverted PSCs is an interlayer able to extract electrons from the active layer to the indium tin oxide (ITO) electrode.[12,13] Commonly used interlayer materials for inverted PSCs include zinc oxide (ZnO),[14,15] cesium carbonate (Cs_2CO_3),[16,17] titanium oxide (TiO_x),[18] titanium chelate,[19] water-/alcohol-soluble conjugated polymers (WSCPs),[3,20−23] and water-/alcohol-soluble nonconjugated polymers.[24] One outstanding example of such inverted PSCs was developed through the combination of a poly[4,8-bis(2-ethylhexyloxyl)-benzo[1,2-b:4,5-b′]dithio-phene-2,6-diyl-*alt*-ethylhexyl-3-fluorothithieno[3,4-*b*]thiophene-2-carboxylate-4,6-diyl] (PTB7, Scheme 1) and (6,6)- phenyl-C71-butyric acid methyl ester ($PC_{71}BM$, Scheme 1) blend active layer and a WSCP interlayer of Poly[9,9-bis(6′- (*N*,*N*-diethylamino)propyl)-fluorene] (PFN).[3] Although this was an important achievement in the PSC field, there is ongoing debate over the fundamental mechanisms by which PFN, or WSCP materials in general, enhance the performance of PSCs. Most previous reports ascribed the performance enhancement to WSCP materials' reduction of the cathode work function (WF) through the formation of interfacial dipoles at the cathode interface.[20−28] This hypothesis is somewhat debatable, however, as the same dipole theory has been used to explain these materials' functions in both organic light-emitting diodes (OLEDs) and PSCs. As OLEDs and PSCs have opposing charge injection/transporting directions, it could be argued that the dipoles introduced by WSCP materials would have opposite effects on OLED and PSC performance. Hence, the dipole theory alone appears insufficient to explain the function of WSCP materials in the aforementioned high-efficiency PSCs. Further complicating the issue is that PFN has non-negligible solubility in the solvent used to process the active layer of PSCs (e.g.,

Received: April 1, 2014
Accepted: June 13, 2014
Published: June 13, 2014

Scheme 1. (a) Devices Configuration of Inverted Polymer Solar Cells; (b) Chemical Structure of PFN-OX and Light Absorption Materials Used in This Study

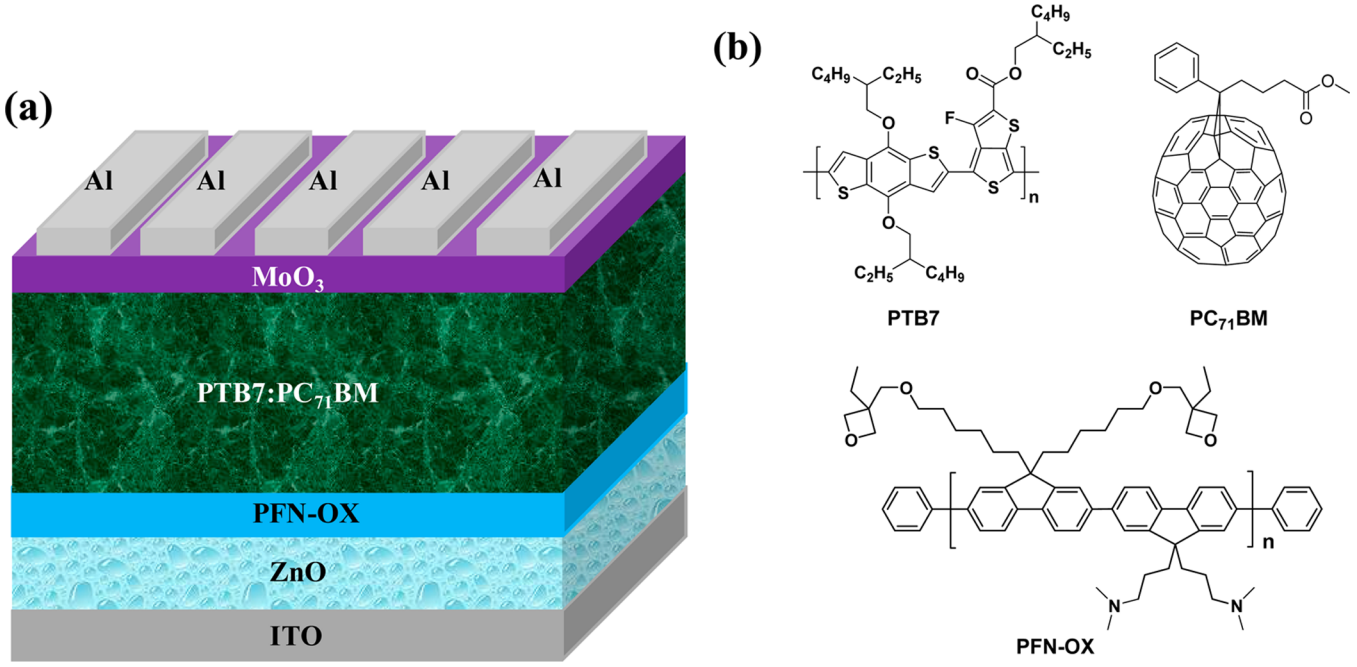

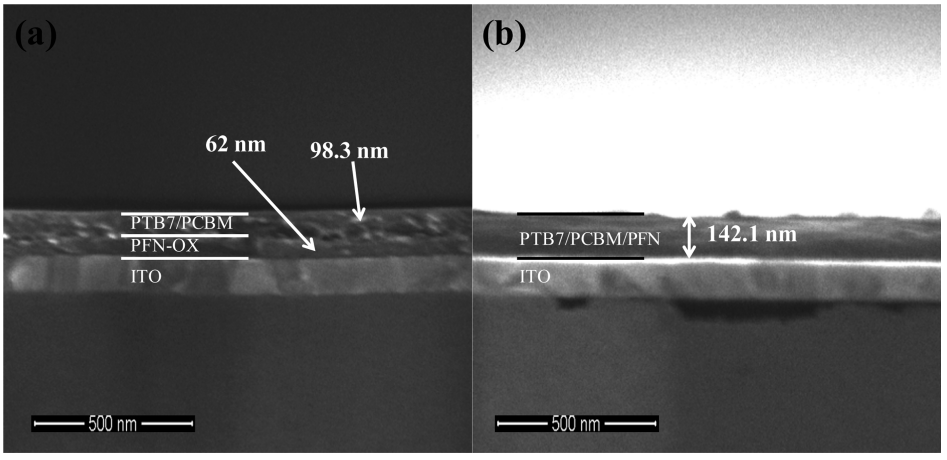

Figure 1. Cross-section SEM images of (a) ITO/PFN-OX/PTB7:$PC_{71}BM$ and (b) ITO/PFN/PTB7:$PC_{71}BM$.

chlorobenzene),[29,30] which makes it difficult to investigate the working mechanism of the PFN interlayer in inverted PSCs, as the ITO/PFN/active-layer stack has poorly defined interfaces. The partially dissolved PFN interlayer may also have a negative effect on further optimizing and increasing PSC efficiency.

In this paper, we report a cross-linkable WSCP material, poly[9,9-bis(6′-(*N*,*N*-diethylamino)propyl)-fluorene-*alt*-9,9-bis-(3-ethyl(oxetane-3-ethyloxy)-hexyl)-fluorene] (PFN-OX, Scheme 1), suitable for inverted PSC applications. What differentiates PFN-OX from PFN is that it can be thermally cross-linked and becomes insoluble in the processing solvent of the active layer. Notes that, the −OX groups are chemically bonded on the end of the side chains, and do not affect the PFN-OX's energy and band structure. This new interlayer material allows us to better understand the detailed working mechanisms of high-efficiency inverted PSCs based on WSCP interlayer materials and PTB7:$PC_{71}BM$ active layers. We found that the PFN-OX interlayer acts as both an electron-extracting, and hole-blocking interlayer for PTB7:$PC_{71}BM$-based PSCs. More importantly, we found PFN-OX has a strong doping effect on $PC_{71}BM$ at the PFN-OX/active-layer interface, which cause its excellent electron-extraction property. These important findings helped us to understand the working mechanism of WASPs and further optimize its hole blocking property in inverted PSCs based on PTB7:$PC_{71}BM$ by introducing ZnO layer, and we were ultimately able to achieve high-efficiency PSCs with a PCE of 9.28% and a high fill factor (FF) of 74.4%.

RESULTS AND DISCUSSION

To investigate the solvent resistance property of the cross-linked PFN-OX thin film, we washed the cross-linked and uncross-linked PFN-OX by spin-casting pristine chlorobenzene onto the thin films and the thickness variations of the resulting films were monitored by optical absorption measurement. It is clear shown (see Figure S1 in the Supporting Information) that cross-linking greatly improved the solvent resistance of PFN-

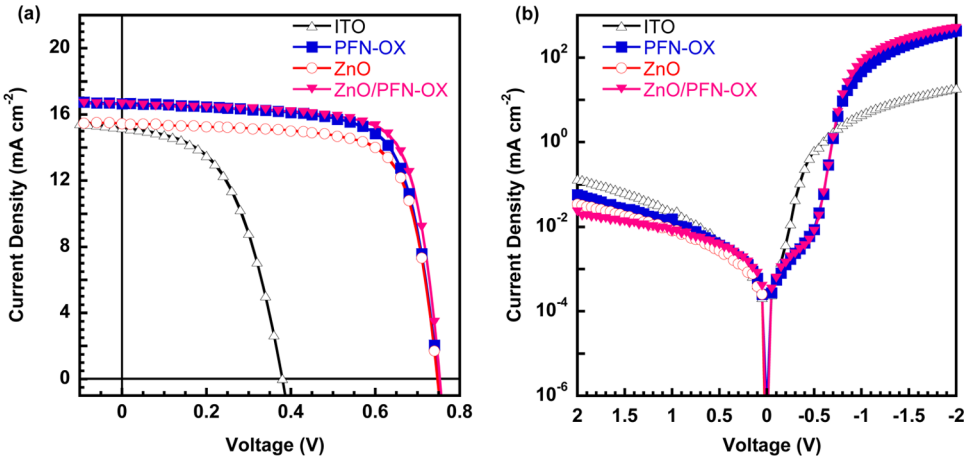

Figure 2. $J-V$ characteristics of inverted PSCs with ITO, ITO/PFN-OX, ITO/ZnO, and ITO/ZnO/PFN-OX as cathodes (a) under illumination and (b) in dark.

Table 1. Photovoltaic Performance of PTB7:$PC_{71}BM$-Based Inverted PSCs with ITO, ITO/PFN-OX, ITO/ZnO and ITO/ZnO/PFN-OX as Cathodes

active layer	cathode	J_{sc} (mA cm^{-2})	V_{oc} (V)	FF (%)	PCE (%)	R_s (Ω)	R_{sh} (Ω)
PTB7:$PC_{71}BM$	ITO	15.41	0.38	52.1	3.05	40	1800
	ITO/PFN-OX	16.65 ± 0.35	0.75 ± 0.01	72.0 ± 0.5	8.99 ± 0.14	24 ± 4	5387 ± 2018
	ITO/ZnO	15.43 ± 0.27	0.75 ± 0.01	73.0 ± 0.6	8.45 ± 0.20	43 ± 6	11587 ± 1872
	ITO/ZnO/PFN-OX	16.63 ± 0.19	0.75 ± 0.01	74.4 ± 0.8	9.28 ± 0.15	13 ± 4	13473 ± 1434

*:Statistic data achieved from 7 independent devices.

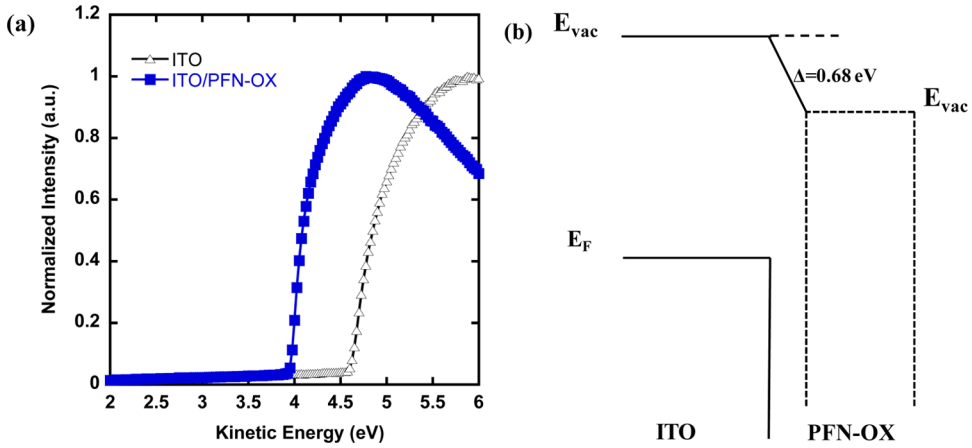

Figure 3. (a) UPS secondary cutoff of ITO substrates with or without a PFN-OX layer on top. (b) Schematic energy levels of the inverted devices under flat conditions.

OX thin film. 70% of the non-cross-linked PFN-OX thin film was washed away by chlorobenzene, while no obvious changes were observed for cross-linked PFN-OX films after washing. Moreover, the interface properties between the PTB7:$PC_{71}BM$ active layer and PFN-OX (or PFN) interlayers were investigated by cross-section scanning electron microscope (SEM). As shown in Figure 1, there is no clear interface observed between PFN and PTB7:$PC_{71}BM$ layers because of the severe interface erosion, whereas the cross-linked PFN-OX offered a more defined interface between PTB7:$PC_{71}BM$ and PFN-OX.

As shown in Figure 2a and Table 1, the open circuit voltage (V_{oc}) of the PSC device increased from 0.38 to 0.75 V, short circuit current density (J_{sc}) was also increased from 15.41 to 16.65 mA cm^{-2}, FF increased from 52.1% to 72.0% after the insertion of PFN-OX between ITO and the active layer, thus, a PCE of 8.99% was achieved. As a comparison, devices with PFN and ZnO as cathode interlayer were also fabricated. ZnO-based devices exhibited a PCE of 8.45%, whereas PFN-based devices exhibited a comparable device performance (PCE = 9.03%) with PFN-OX based device (PCE = 8.99%), which means the cross-linking procedure did not destroy the cathode modification ability of PFN-OX.

Our mechanism study of how the PFN-OX interlayer functions inside an inverted PSC device consisted of several parts. First, ultraviolet photoelectron spectroscopy (UPS) was used to investigate the WF change on ITO substrates with and without PFN-OX modification. As shown in Figure 3, the WF shifted from 4.63 to 3.95 eV upon ITO modification with PFN-OX. The ~0.7 eV shift in the ITO WF introduced by PFN-OX

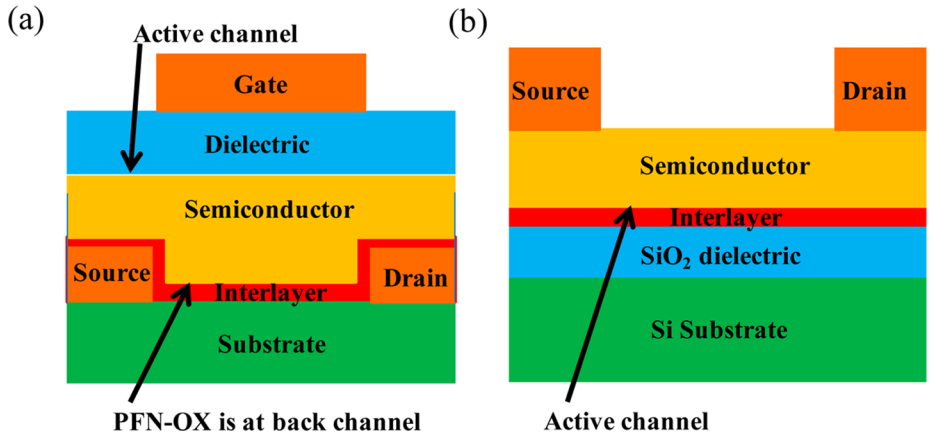

Figure 4. Structures of (a) BCTG OFET and (b) BGTC OFET.

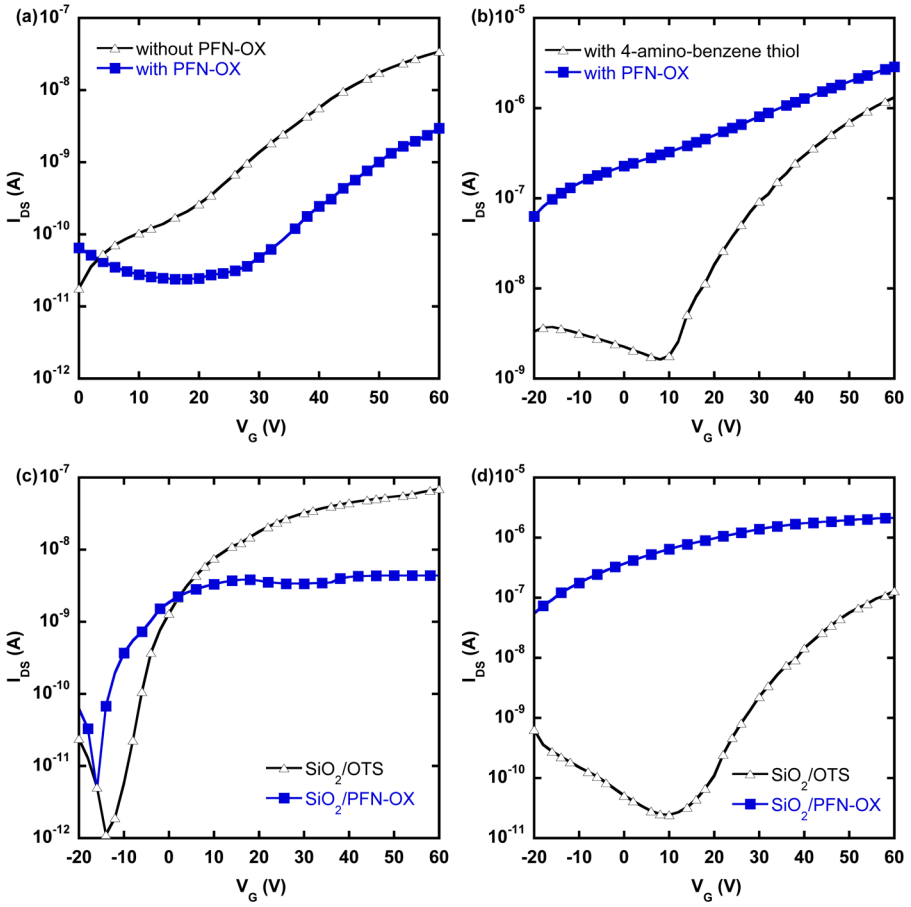

Figure 5. Transfer plots of (a) PTB7-based and (b) $PC_{71}BM$-based BCTG OFETs; (c) PTB7-based and (d) $PC_{71}BM$-based BGTC OFETS.

is similar to the value reported in the case of PFN,[3] which suggests that the cross-linking process does not influence the WF tuning function of WSCP materials. The reduced WF of ITO increased the built-in potential of the inverted PSCs. Thus, increased V_{oc} was observed in the inverted PSC device relative to the reference device without PFN-OX.

Second, a series of experiments were carried out to better understand the electron-extraction and hole-blocking functions of the PFN-OX interlayer at the ITO/active layer interface. The concepts of electron transport and a hole-blocking layer (HBL) or hole transport and an electron-blocking layer had been widely explored in the OLED and small molecule-based organic photovoltaic (SM-OPV) fields,[31,32] but it remains unclear whether the reported WSCP materials had the functions of a typical HBL. The first evidence of PFN-OX's electron-extraction and hole-blocking property was found in the dark current density−voltage (J−V) curve (Figure 2b) of the PFN-OX-based PSCs, which clearly showed an increased current in the forward direction and reduced current in the reverse direction. Also, the series resistance of the PFN-OX-based devices decreased and the shunt resistance increased upon the insertion of PFN-OX between ITO and the active layer (Table 1). To further explore PFN-OX's electron-extraction and hole-blocking functions, bottom-contact top-gate (BCTG) organic

dx.doi.org/10.1021/am501920z | ACS Appl. Mater. Interfaces 2014, 6, 10429−10435

field-effect transistor (OFET, Figure 4a) devices were fabricated using PFN-OX as the interlayer. In such BCTG OFET structures, charges (either electrons or holes) are injected from the source electrode, via PFN-OX, to the semiconductor layer and then extracted from that layer to the drain electrode via PFN-OX again. As shown in Figure 5a, the insertion of PFN-OX at the electrode/semiconductor interface reduced the I_{ds} of the p-channel OFET devices based on PTB7, which indicates that PFN-OX has at least moderate hole-blocking properties. Figure 5b shows the transfer plots of two $PC_{71}BM$-based n-channel OFET devices with a PFN-OX interlayer or a 4-amino-benzenethiol interlayer. The I_{ds} of the OFET device with the PFN-OX interlayer underwent a dramatic increase compared to that with the 4-amino-benzenethiol interlayer. Although the 4-amino-benzenethiol interlayer already constitutes a strong electron-injection interlayer,[33] the PFN-OX interlayer appears to have an even stronger effect in enhancing the electron injection/extraction between the electrodes and semiconductor layer. This evidence, combined with the previous dark $J-V$ data, strongly supports the proposition that the PFN-OX interlayer has excellent electron-injection/-extraction properties and at least moderate hole-blocking properties. Note that OFET operation involves both electron injection (at the source electrode) and electron extraction (at the drain electrode) processes. Therefore, our OFET data indicate that PFN-OX is capable of both injecting electrons into and extracting them from $PC_{71}BM$.

Further experiments show that PFN-OX's electron-injection/-extraction properties are not solely caused by interfacial dipole formation, but may also be influenced by electron doping effect of PFN-OX on $PC_{71}BM$ at the interface. As shown in Figure 5b, the PFN-OX-based OFETs exhibited a higher I_{off} and lower on/off ratio than the reference device, which led us to speculate that PFN-OX has a doping effect on $PC_{71}BM$. As previous research has shown that the surface chemistry of the back channel to exert a significant influence on the I_{off} of OFET devices,[34] the higher I_{off} of that in Figure 5b indicates that there is a doping effect between PFN-OX and $PC_{71}BM$. To further confirm this doping effect, we also fabricated bottom-gate top-contact (BGTC) OFETs (Figure 4b) with the PFN-OX interlayer. Note that the BGTC OFETs in Figure 4b have an inverted structure compared to the BCTG OFETs in Figure 4a. The difference is this: in the BCTG OFETs, PFN-OX is not located at the active channel (the active channel is the dielectric/semiconductor interface, and PFN- OX is located at the substrate/semiconductor interface, referred to as the back channel), whereas in the BGTC OFETs, it is. Therefore, PFN-OX's doping effect on $PC_{71}BM$ should exert a stronger influence on the I_{ds} than in the BCTG OFET case. Figure 5d shows that the PFN-OX-based BGTC OFETs are heavily doped, with the I_{off} 3 orders of magnitude greater than that in the OFET device without the PFN-OX interlayer. These data provide an additional support for our hypothesis that PFN-OX has a doping effect on $PC_{71}BM$. At the same time, for similar BGTC OFETs with PTB7 as the semiconductor layer, the device with the PFN-OX interlayer displayed a significantly reduced current compared to the device without this interlayer in Figure 5c, which suggest that PFN-OX acts as a hole trap[35] for p-channel OFETs, thus proving a partial explanation for its possession of hole-blocking properties.

Encouragingly, similar phenomena were independently reported by Bao's and Jen's groups recently, who obtained highly conductive fullerenes through doping.[36−38] Chen et al. found there is a significant electron transfer from PFN-modified ITO to C_{60} through electron tunnelling, as revealed by in situ UPS measurements,[39] whereas in this work, the FET study results indicate that the charge transfer occurred from PFN-OX itself to PCBM. Now, it is quite clear that doping of $PC_{71}BM$ is the major reason for its enhancement of electron injection/extraction across the ITO/active layer interface. Interfacial doping has been widely used to reduce contact resistance and to enhance charge injection in SM-OLEDs, SM-OPVs, inorganic solar cells, and the like. The insertion of a doped interlayer between the electrode and nondoped semiconductor layer can help to form an ohmic contact at the electrode/semiconductor interface, which then facilitates either charge injection (for OLEDs) or charge extraction (for solar cells).[40] We believe that the elucidation of interfacial doping in high-efficiency PSCs presented herein will have a significant influence of PSCs research.

Such elucidation allows us to better understand the device performance of PSCs based on the PFN-OX interlayer. This enhanced V_{oc} was the result of the reduced WF of ITO and thus increased built-in potential of the device upon the addition of the PFN-OX interlayer. The increase in J_{sc} can be attributed, among other factors, to the doping effect of PFN-OX on $PC_{71}BM$, as a doped interface can help to extract more electrons from the active layer. The FF increase can be explained by the better rectification characteristics of the dark $J-V$ curve (Figure 2b) and the electron-extracting and hole-blocking properties of the PFN-OX interlayer. It should be noted that PFN-OX also exhibited excellent devices performance in other polymer/fullerene systems besides PTB7.[5,41] It is important to note that PFN-OX exhibited excellent electron-injection/-extraction properties but only moderate hole-blocking ability, as the hole current (Figure 5c) in the PTB7-based OFETs was reduced by the insertion of the PFN-OX interlayer, but not completely eliminated. In an attempt to increase the hole-blocking ability of PFN-OX, we increased the thickness of the PFN-OX layer, but found that it reduced PSC performance because a thicker PFN-OX interlayer increases PSC series resistance.[11] PFN-OX works particularly well in enhancing electron injection/extraction not because of the high electron conductivity of the bulk material, but because of its doping effect on $PC_{71}BM$ at the interface. PFN-OX must thus be kept at a low thickness level to minimize its bulk resistance while utilizing its interfacial doping effect on $PC_{71}BM$. We thus needed to improve the hole-blocking ability of the PFN-OX interlayer without increasing its thickness or sacrificing its electron-extraction properties. To do so, we added an additional ZnO interlayer between the ITO and PFN-OX to form a double-layer interlayer. As shown in Figure 2b, this double-layer interlayer further improved the rectification characteristics of the dark $J-V$ curve of the inverted PSCs, indicative of its greater hole-blocking and electron-extraction ability. As a result, the FF of the PSCs increased from 72.0 to 74.4%. Because the ohmic contact has been achieved in ZnO[42] and PFN-OX based devices, the devices based on ZnO, PFN-OX and ZnO/PFN-OX interlayers exhibited similar V_{oc}, whereas the PFN-OX and ZnO/PFN-OX-based devices showed higher J_{sc} than that of ZnO-based device because of the interfacial doping of PCBM by PFN-OX. Consequently, the PCE of ZnO/PFN-OX-based device was thus improved to 9.28%.

CONCLUSIONS

To summarize, we have developed a cross-linkable WSCP material called PFN-OX. The cross-linkable nature of PFN-OX allowed us to fabricate inverted PSCs with well-defined interfaces and to investigate the detailed working mechanism of high-efficiency inverted PSCs based on PTB7:$PC_{71}BM$ active layers. We found the PFN-OX interlayer to exhibit excellent electron-extraction and moderate hole-blocking properties at the ITO/active layer interface. PFN-OX's excellent ability to enhance electron extraction from the active layer to the ITO electrode attributed to the combination of two effects: ITO's decreased WF upon PFN-OX surface modification and PFN-OX's strong doping effect on $PC_{71}BM$. Inspired by this understanding, we further improved the hole-blocking ability of the PFN-OX interlayer by inserting a thin layer of ZnO between the ITO and PFN-OX. The resulting ZnO/PFN-OX-based PSCs achieved an impressive FF of 74.4% and PCE of 9.28%. This paper provides a detailed picture of how WSCP materials function inside high-efficiency inverted PSC devices, and thus offers important guidance for the design and optimization of these materials for high-efficiency inverted PSCs.

EXPERIMENTAL SECTION

Inverted PSC Fabrication and Measurements. ITO substrates were rinsed with standard procedure. Ten nm ZnO thin films coated ITO substrates were obtained according to reported literature.[43] Then, PFN-OX was spin-coated onto ITO or ITO/ZnO substrates from its methanol:acetic acid (100:1 v/v) solution to achieve ~5 nm interlayer and heated at 150 °C for 20 min to finish the cross-linking. The PTB7:$PC_{71}BM$ (1:1.5 w/w) active layer was prepared by spin-coating a mixed solvent of chlorobenzene/1,8-diiodoctane (100:3 v/v) solution with concentration of 11 mg/mL, the thickness was 100 nm. Finally, a 10 nm MoO_3 and 100 nm Al were thermally evaporated as anode through a shadow mask (active area was defined) in a vacuum chamber with a base pressure of 1×10^{-6} mbar. The current density–voltage (J–V) curves were measured on a computer-controlled Keithley 2400 sourcemeter under 1 sun, AM 1.5 G spectrum from a class solar simulator (Japan, SAN-EI, XES-40S1), the light intensity was 100 mW/cm^2 as calibrated by a Newport certified reference silicon cell (PV Measurements, with KG-5 visible filter). Spectral mismatch factors (M) value of 1.03 was used to obtain the correct photocurrent and efficiency for the devices according to previously published paper,[3] where the measurement condition are identical. The IPCE spectra were performed on a commercial IPCE measurement system (Beijing, Zolix, DSR 100UV–B).

ASSOCIATED CONTENT

Supporting Information

Active layer materials, synthesis of PFN-OX, UPS study, and OFET devices fabrication. Figure S1, absorption spectra of PFN-OX thin films with different cross-linking conditions. Figure S2, IPCE spectrum of inverted PSCs with ITO, ITO/PFN-OX, ITO/ZnO, and ITO/ZnO/PFN-OX as cathodes. Table S1, calculated J_{sc} according to IPCE spectrum. This material is available free of charge via the Internet at http://pubs.acs.org.

AUTHOR INFORMATION

Corresponding Authors

*E-mail: msfhuang@scut.edu.cn.
*E-mail: hyan@ust.hk.

Notes

The authors declare no competing financial interest.

ACKNOWLEDGMENTS

The work was financially supported by the Ministry of Science and Technology (2014CB643501), the Natural Science Foundation of China (21125419 and 51361165301) and Guangdong Natural Science Foundation (Grant S2012030006232). He Yan, Cheng Mu, Zhengke Li acknowledge Hong Kong ITC for financial support through project ITS/354/12 and Hong Kong RGC through project N_HKUST623/13.

REFERENCES

(1) Yu, G.; Gao, J.; Hummelen, J. C.; Wudl, F.; Heeger, A. J. Polymer Photovoltaic Cells: Enhanced Efficiencies via a Network of Internal Donor-Acceptor Heterojunctions. *Science* **1995**, *270*, 1789–1791.
(2) Li, G.; Zhu, R.; Yang, Y. Polymer Solar Cells. *Nat. Photonics.* **2012**, *6*, 153–161.
(3) He, Z.; Zhong, C.; Su, S.; Xu, M.; Wu, H.; Cao, Y. Enhanced Power-Conversion Efficiency in Polymer Solar Cells Using an Inverted Device Structure. *Nat. Photonics.* **2012**, *6*, 591–595.
(4) Gupta, V.; Kyaw, A.; Wang, D.; Chand, S.; Bazan, G. C.; Heeger, A. J. Barium: An Efficient Cathode Layer for Bulk-Heterojunction Solar Cells. *Sci. Rep.* **2013**, *3*, 1965.
(5) Guo, X.; Zhang, M.; Ma, W.; Ye, L.; Zhang, S.; Liu, S.; Ade, H.; Huang, F.; Hou, J. Enhanced Photovoltaic Performance by Modulating Surface Composition in Bulk Heterojunction Polymer Solar Cells Based on PBDTTT-C-T/$PC_{71}BM$. *Adv. Mater.* **2014**, DOI: 10.1002/adma.201400411.
(6) You, J.; Dou, L.; Yoshimura, K.; Kato, T.; Ohya, K.; Moriarty, T.; Emery, K.; Chen, C.; Gao, J.; Li, G.; Yang, Y. A Polymer Tandem Solar Cell with 10.6% Power Conversion Efficiency. *Nat. Commun.* **2013**, *4*, 1446.
(7) Liu, Y.; Chen, C.; Hong, Z.; Gao, J.; Yang, Y.; Zhou, H.; Dou, L.; Li, G.; Yang, Y. Solution-Processed Small-Molecule Solar Cells: Breaking the 10% Power Conversion Efficiency. *Sci. Rep.* **2013**, *3*, 3356.
(8) Chen, L.-M.; Hong, Z.; Li, G.; Yang, Y. Recent Progress in Polymer Solar Cells: Manipulation of Polymer:Fullerene Morphology and the Formation of Efficient Inverted Polymer Solar Cells. *Adv. Mater.* **2009**, *21*, 1434–1449.
(9) Hau, S. K.; Yip, H.-L.; Jen, A. K.-Y. A Review on the Development of the Inverted Polymer Solar Cell Architecture. *Polym. Rev.* **2010**, *50*, 474–510.
(10) Jørgensen, M.; Norrman, K.; Gevorgyan, S. A.; Tromholt, T.; Andreasen, B.; Krebs, F. C. Stability of Polymer Solar Cells. *Adv. Mater.* **2012**, *24*, 580–612.
(11) Liu, S.; Zhang, K.; Lu, J.; Zhang, J.; Yip, H.-L.; Huang, F.; Cao, Y. High-Efficiency Polymer Solar Cells via the Incorporation of an Amino-Functionalized Conjugated Metallopolymer as a Cathode Interlayer. *J. Am. Chem. Soc.* **2013**, *135*, 15326–15329.
(12) Steim, R.; Kogler, F. R.; Brabec, C. J. Interface Materials for Organic Solar Cells. *J. Mater. Chem.* **2010**, *20*, 2499–2512.
(13) Yip, H.-L.; Jen, A. K.-Y. Recent Advances in Solution-Processed Interfacial Materials for Efficient and Stable Polymer Solar Cells. *Energy Environ. Sci.* **2012**, *5*, 5994–6011.
(14) White, M. S.; Olson, D. C.; Shaheen, S. E.; Kopidakis, N.; Ginley, D. S. Inverted Bulk-Heterojunction Organic Photovoltaic Device Using a Solution-Derived ZnO Underlayer. *Appl. Phys. Lett.* **2006**, *89*, 143517.
(15) Sun, Y.; Seo, J. H.; Takacs, C. J.; Seifter, J.; Heeger, A. J. Inverted Polymer Solar Cells Integrated with a Low-Temperature-Annealed Sol-Gel-Drived ZnO Film as an Electron Transport Layer. *Adv. Mater.* **2011**, *23*, 1679–1683.
(16) Li, G.; Chu, C.-W.; Shrotriya, V.; Huang, J.; Yang, Y. Efficient Inverted Polymer Solar Cells. *Appl. Phys. Lett.* **2006**, *88*, 253503.
(17) Liao, H.-H.; Chen, L.-M.; Xu, Z.; Li, G.; Yang, Y. Highly Efficient Inverted Polymer Solar Cell by Low Temperature Annealing of Cs_2CO_3 Interlayer. *Appl. Phys. Lett.* **2008**, *92*, 173303.

(18) Waldauf, C.; Morana, M.; Denk, P.; Schilinsky, P.; Coakley, K.; Choulis, S. A.; Brabec, C. J. Highly Efficient Inverted Organic Photovoltaics Using Solution Based Titanium Oxide as Electron Selective Contact. *Appl. Phys. Lett.* **2006**, *89*, 233517.
(19) Tan, Z.; Zhang, W.; Zhang, Z.; Qian, D.; Huang, Y.; Hou, J.; Li, Y. High-Performance Inverted Polymer Solar Cells with Solution-Processed Titanium Chelate as Electron-Collecting Layer on ITO electrode. *Adv. Mater.* **2012**, *24*, 1476−1481.
(20) Na, S.-I.; Kim, T.-S.; Oh, S.-H.; Kim, J.; Kim, S.-S.; Kim, D.-Y. Enhanced Performance of Inverted Polymer Solar Cells with Cathode Interfacial Tuning via Water-Soluble Polyfluorenes. *Appl. Phys. Lett.* **2010**, *97*, 223305.
(21) Zilberberg, K.; Behrendt, A.; Kraft, M.; Scherf, U.; Riedl, T. Ultrathin Interlayers of a Conjugated Polyelectrolyte for Low Work-Function Cathodes in Efficient Inverted Organic Solar Cells. *Org. Electron.* **2013**, *14*, 951−957.
(22) Huang, F.; Wu, H.; Cao, Y. Water/Alcohol Soluble Conjugated Polymers as Highly Efficient Electron Transporting/Injection Layer in Optoelectronic Devices. *Chem. Soc. Rev.* **2010**, *39*, 2500−2521.
(23) Duan, C.; Zhang, K.; Zhong, C.; Huang, F.; Cao, Y. Recent Advances in Water/Alcohol-Soluble π-Conjugated Materials: New Materials and Growing Applications in Solar Cells. *Chem. Soc. Rev.* **2013**, *42*, 9071−9104.
(24) Zhou, Y.; Fuentes-Hernandez, C.; Shim, J.; Meyer, J.; Giordano, A. J.; Li, H.; Winget, P.; Papadopoulos, T.; Cheum, H.; Kim, J.; Fenoll, M.; Dindar, A.; Haske, W.; Najafabadi, E.; Khan, T. M.; Sojoudi, H.; Barlow, S.; Graham, S.; Brédas, J.-L.; Marder, S. R.; Kahn, A.; Kippelen, B. A Universal Method to Produce Low-Work Function Electrodes for Organic Electronics. *Science* **2012**, *336*, 327−332.
(25) He, Z.; Zhong, C.; Huang, X.; Wong, W.-Y.; Wu, H.; Chen, L.; Su, S.; Cao, Y. Simultaneous Enhancement of Open-Circuit Voltage, Short-Circuit Current Density, and Fill Factor in Polymer Solar Cells. *Adv. Mater.* **2011**, *23*, 4636−4643.
(26) Oh, S.-H.; Na, S.-I.; Jo, J.; Lim, B.; Vak, D.; Kim, D.-Y. Water-Soluble Polyfluorenes as an Interfacial Layer Leading to Cathode-Independent High Performance of Organic Solar Cells. *Adv. Funct. Mater.* **2010**, *20*, 1977−1983.
(27) Shi, T.; Zhu, X.; Yang, D.; Xie, Y.; Zhang, J.; Tu, G. Thermal Annealing Influence on Poly(3-hexyl-thiophene)/phenyl-C61-butyric acid methyl ester-Based Solar Cells with Anionic Conjugated Polyelectrolyte as Cathode Interface Layer. *Appl. Phys. Lett.* **2012**, *101*, 161602.
(28) Chen, L.; Xie, C.; Chen, Y. Influences of Charge of Conjugated Polymer Electrolytes Cathode Interlayer for Bulk-Heterojunction Polymer Solar Cells. *Org. Electron.* **2013**, *14*, 1551−1561.
(29) Liu, S.; Zhong, C.; Zhang, J.; Duan, C.; Wang, X.; Huang, F. A Novel Crosslinkable Electron Injection/Transporting Material for Solution Processed Polymer Light-Emitting Diodes. *Sci. China Chem.* **2011**, *54*, 1745−1749.
(30) Zhong, C.; Liu, S.; Huang, F.; Wu, H.; Cao, Y. Highly Efficient Electron Injection from Indium Tin Oxide/Cross-Linkable Amino-Functionalized Polyfluorene Interface in Inverted Organic Light Emitting Devices. *Chem. Mater.* **2011**, *23*, 4870−4876.
(31) Adamovich, V. I.; Cordero, S. R.; Djurovich, P. I.; Tamayo, A.; Thompson, M. E.; D'Andrade, B. W.; Forrest, S. R. New Charge-Carrier Blocking Materials for High Efficiency OLEDs. *Org. Electron.* **2003**, *4*, 77−87.
(32) Li, N.; Lassiter, B. E.; Lunt, R. R.; Wei, G.; Forrest, S. R. Open Circuit Voltage Enhancement Due to Reduced Dark Current in Small Molecule Photovoltaic Cells. *Appl. Phys. Lett.* **2009**, *94*, 023307.
(33) Kitamura, M.; Kuzumoto, Y.; Aomori, S.; Kamura, M.; Na, J. H.; Arakawa, Y. Threshold Voltage Control of Bottom-Contact *n*-Channel Organic Thin-Film Transistors Using Modified Drain/Source Electrodes. *Appl. Phys. Lett.* **2009**, *94*, 083310.
(34) Boudinet, D.; Benwadih, M.; Altazin, S.; Verilhac, J.-M.; Vito, E. D.; Serbutoviez, C.; Horowitz, G.; Facchetti, A. Influence of Substrate Surface Chemistry on the Performance of Top-Gate Organic Thin-Film Transistors. *J. Am. Chem. Soc.* **2011**, *133*, 9968−9971.
(35) Duan, C.; Cai, W.; Hsu, B. B. Y.; Zhong, C.; Zhang, K.; Liu, C.; Hu, Z.; Huang, F.; Bazan, G. C.; Heeger, A. J.; Cao, Y. Toward Green Solvent Processable Photovoltaic Materials for Polymer Solar Cells: the Role of Highly Polar Pendant Groups in Charge Carrier Transport and Photovoltaic Behavior. *Energy Environ. Sci.* **2013**, *6*, 3022−3034.
(36) Wei, P.; Menke, T.; Naab, B. D.; Leo, K.; Riede, M.; Bao, Z. 2-(2-Methoxyphenyl)-1,3-dimethyl-1*H*-benzoimidazol-3-ium Iodide as a New Air-Stable n-Type Dopant for Vacuum-Processed Organic Semiconductor Thin Films. *J. Am. Chem. Soc.* **2012**, *134*, 3999−4002.
(37) Li, C.-Z.; Chueh, C.-C.; Yip, H.-L.; Ding, F.; Li, X.; Jen, A. K.-Y. Solution-Processible Highly Conducting Fullerenes. *Adv. Mater.* **2013**, *25*, 2457−2461.
(38) Cho, N.; Li, C.-Z.; Yip, H.-L.; Jen, A. K.-Y. In situ Doping and Crosslinking of Fullerenes to Form Efficient and Robust Electron-Transporting Layers for Polymer Solar Cells. *Energy Environ. Sci.* **2014**, *7*, 638−643.
(39) Zhong, S.; Wang, R.; Mao, H.; He, Z.; Wu, H.; Chen, W.; Cao, Y. Interface Investigation of the Alcohol-/Water-Soluble Conjugated Polymer PFN as Cathode Interfacial Layer in Organic Solar Cells. *J. Appl. Phys.* **2013**, *114*, 113709.
(40) Walzer, K.; Maennig, B.; Pfeiffer, M.; Leo, K. Highly Efficient Organic Devices Based on Electrically Doped Transport Layers. *Chem. Rev.* **2007**, *107*, 1233−1271.
(41) Dong, Y.; Hu, X.; Duan, C.; Liu, P.; Liu, S.; Lan, L.; Chen, D.; Ying, L.; Su, S.; Gong, X.; Huang, F.; Cao, Y. A Series of New Medium-Bandgap Conjugated Polymers Based on Naphtho[1,2-c:5,6-c]bis(2-octyl-[1,2,3]triazole) for High-Performance Polymer Solar Cells. *Adv. Mater.* **2013**, *25*, 3683−3688.
(42) Chang, Y.-M.; Leu, C.-Y. Conjugated Polyelectrolyte and Zinc Oxide Stacked Structure as an Interlayer in Highly Efficient and Stable Organic Photovoltaic Cells. *J. Mater. Chem. A* **2013**, *1*, 6446−6451.
(43) Yang, T.; Cai, W.; Qin, D.; Wang, E.; Lan, L.; Gong, X.; Peng, J.; Cao, Y. Solution-Processed Zinc Oxide Thin Film as a Buffer Layer for Polymer Solar Cells with an Inverted Device Structure. *J. Phys. Chem. C* **2010**, *114*, 6849−6853.